JOURNAL OF AGRICULTURAL AND FOOD CHEMISTRY

Influence of Storage Conditions on the Structure, Thermal Behavior, and Formation of Enzyme-Resistant Starch in Extruded Starches

HÉLÈNE CHANVRIER,[†] SURJANI UTHAYAKUMARAN,[†] INGRID A. M. APPELQVIST,[†] MICHAEL J. GIDLEY,[‡] ELLIOT P. GILBERT,[§] AND AMPARO LÓPEZ-RUBIO*[,§]

Commonwealth Scientific and Industrial Research Organisation, Food Futures National Research Flagship and CSIRO, Food Science Australia, Riverside Corporate Park, North Ryde, New South Wales 2213, Australia, Centre for Nutrition and Food Sciences, University of Queensland, St. Lucia, Queensland 4072, Australia, and Bragg Institute, Australian Nuclear Science and Technology Organization, PMB 1, Menai, New South Wales 2234, Australia

Starch structures from an extrusion process were stored at different temperatures to allow for molecular rearrangement (retrogradation); their thermal characteristics (DSC) and resistance to amylase digestion were measured and compared. The structure of four native and processed starches containing different amylose/amylopectin compositions (3.5, 30.8, 32, and 80% amylose content, respectively) before and after digestion was studied with small-angle X-ray scattering (SAXS) and X-ray diffraction (XRD). Rearrangement of the amylose molecules was observed for each storage condition as measured by the DSC endotherm at around 145 °C. The crystalline organization of the starches after processing and storage was qualitatively different to that of the native starches. However, there was no direct correlation between the initial crystallinity and the amount of enzyme-resistant starch (ERS) measured after *in vitro* digestion, and only in the case of high-amylose starch did the postprocess conditioning used lead to a small increase in the amount of starch remaining after the enzymatic treatment. From the results obtained, it can be concluded that retrograded amylose is not directly correlated with ERS and alternative mechanisms must be responsible for ERS formation.

KEYWORDS: Enzyme-resistant starch; extrusion; XRD; DSC; SAXS; structure; functional food

INTRODUCTION

The importance of starch in the human diet arises from being one of the main constituents of native and processed foods. The wide variety of starch sources with different compositions and characteristics provide this complex polysaccharide with great versatility to match specific product requirements.

The existence of a starch fraction, known as "resistant starch", that is not readily digested in the small intestine is not a new concept; however, in recent years, many studies have focused on this "functional" ingredient because of the current changes in consumption habits involving an increase in energy intake with its associated influence on obesity and diet-associated disorders, such as diabetes (*1*). The increasing consumer health consciousness and the growing demand for healthy foods are stimulating innovation and new product development in the food industry internationally, as reflected in the expanding worldwide interest in functional foods.

Within the range of functional compounds available, resistant starch has been chosen to be a key ingredient in several food products because, apart from being a prebiotic (as this fraction escapes digestion in the small intestine and enters the colon, where it may serve as a growth substrate for intestinal bacteria), it has been demonstrated to have a protective mechanism against colorectal cancer through its fermentation by intestinal bacteria to butyrate (*2*).

Resistant starch (RS) has been classified into four different groups (*3*), with type III corresponding to the resistant fractions present in "starchy" foods that have been processed, cooled, and stored. This RS fraction has been normally ascribed to molecularly reorganized amylose (retrograded amylose), because it has been observed that retrograded amylopectin is completely degraded by α-amylase (*4*). The majority of the studies have been carried out using *in vitro* digestion experiments which, despite differing in detail from digestion in the human gastrointestinal tract, have been designed to simulate *in vivo* conditions. However, information on the structure of starch that escapes digestion remains limited. The fractions remaining after *in vitro* digestion will be termed "enzyme-resistant starch" (ERS) to distinguish them from the products obtained *in vivo* ("physiologically resistant starch" or PRS).

* To whom correspondence should be addressed. Telephone: (61) 2-9717-7273. Fax: (61) 2-9717-3606. E-mail: amparo.lopez.rubio@ansto.gov.au.

[†] Food Science Australia.

[‡] Centre for Nutrition and Food Sciences.

[§] Australian Nuclear Science and Technology Organization.

10.1021/jf071974e CCC: $37.00
Published on Web 10/26/2007

Table 1. Composition of the Raw Starches

starch	moisture content (%)	amylose (%)	lipids (%)
normal maize starch	9.4	30.8	0.2
high-amylose maize starch	10.3	80.0	0.2
waxy maize starch	12.3	3.5	0.1
normal wheat starch	9.1	32.0	0.2

In contrast with the classical aim of processing, mainly intended to increase the digestibility of food, nowadays, such transformation processes are designed to develop tasty and palatable foods with improved functional properties and reduced energy intake. To understand and control the textural attributes and digestibility of starch-based products, it is necessary to determine the structure and physicochemical changes undergone by this biopolymer during processing and storage. During storage, starch is known to recrystallize (a process known as retrogradation), which is a complex process and depends upon many factors, such as the type of starch, starch concentration, cooking and cooling regimes, pH, and the presence of solutes, such as lipids, salts, sugars (*5*), and hydrocolloids (*6*). Current interest in this process is linked with its correlation to increased ERS levels. An increase in the ERS content in extruded starches during storage has been observed to be linked to an increase of the melting enthalpy measured by differential scanning calorimetry (DSC) (*7*). In the case of wet starch systems, if the starch is retrograded or partially gelatinized, a higher resistance to enzyme digestion has been detected (*8*).

For a fixed processing technology, the main factors that determine retrogradation and, therefore, could potentially influence the RS content are the composition of the starch, the product matrix, and the moisture content. In general, high-amylose starches deliver higher RS fractions than their low-amylose starch counterparts (*9*). In terms of moisture content, water acts as a starch plasticizer, decreasing the glass transition temperature (T_g), thus allowing the chains to recrystallize at a lower temperature. Storing the starch samples above their T_g, where the starch chains have increased mobility, could also potentially lead to higher levels of ERS.

The aim of this work was to produce different starch structures through processing and storage using several starch varieties and correlate their structural organization with the enzyme digestibility of the end-products. In this approach, several starch-based products were produced by extrusion processing of starch containing different compositions (normal, waxy, and high amylose) and subsequently stored at various temperatures to favor the rearrangement of the amylose chains. The final products have been analyzed to understand the impact of the initial starch architecture and storage conditions on the product's structural properties and sensitivity to enzyme digestion. Structures of *in vitro* digested starch have also been assessed and compared to the initial structure of the processed products.

MATERIALS AND METHODS

Starch Samples. Four types of starches provided by Penford Australia Ltd. (Australia) were used: normal maize (30.8% amylose), waxy maize (3.5% amylose), high-amylose maize (80% amylose), and normal wheat starch (32% amylose). The amylose content was determined by the iodine-binding method according to Chrastil (*10*). More detailed information on the composition of the different starches is shown in **Table 1**.

Starch Processing. The different starches were processed using a capillary rheometer (Rosand RH2000 Rheometers, Bohlin Instruments Ltd., U.K.). Prior to processing, the moisture content of the raw starches was adjusted to 28% (wet basis) and left in a sealed container at 4 °C overnight. The processing temperature was 140 °C, corresponding to a temperature higher than the melting temperature to fully gelatinize the starch. After thermal equilibration for 1 min at 140 °C, the melt was extruded through an 8 mm die (1 mm in diameter) at a shear rate of 722 s^{-1}.

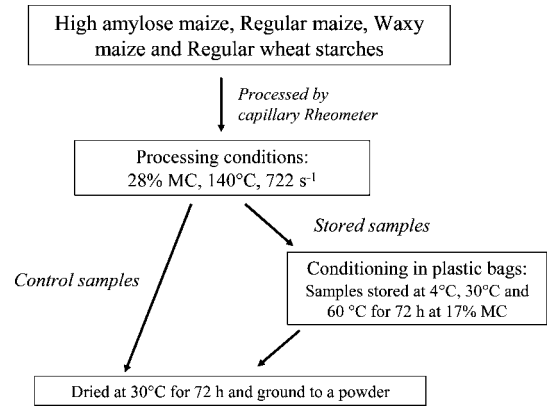

Figure 1. Schematic diagram showing the conditions used for processing and storing the different starch samples.

Material Conditioning. For storage conditioning, the processed samples were sealed in plastic bags and placed in different temperature chambers: 4, 30, and 60 °C for 72 h. The moisture content during conditioning was 17%. After storage, the samples were taken out of the plastic bags and dried at 30 °C for 72 h. Processed control samples were directly dried after processing (30 °C during 72 h) to avoid structural transformations. A schematic diagram illustrating the processing and storage conditions is presented in **Figure 1**.

DSC: Residual Gelatinization Enthalpy and Melting Enthalpy. To check the extent of starch transformation after processing, samples were ground into powder and ~8 mg of starch was placed into the DSC pan with excess water added (40 μL). The scan was carried out immediately after adding the water, to minimize retrogradation, over the range from 20 to 180 at 10 °C/min to observe the presence of any residual gelatinization peak. Two replicates were run for each sample.

X-ray Diffraction (XRD). XRD was carried out on a Panalytical X'Pert Pro diffractometer. The instrument was equipped with a Cu long fine focus tube, programmable incident beam divergence slit and diffracted beam scatter slit (both fixed at 0.125°), and an X'celerator high-speed detector. The samples were examined over the angular range of 2–40° with a step size of 0.0332° and a count time of 800 s per point. Crystallinity determination was carried out using the X'Pert software. This program automatically fits the amorphous background in the diffraction pattern, and the crystallinity is calculated from the intensity ratio of the diffraction peaks (I_{net}) to the sum of all intensity measured (I_{total}).

$$\text{crystallinity (\%)} = 100 \times (I_{net}/I_{total})$$

Small-Angle X-ray Scattering (SAXS). SAXS measurements were performed on a Bruker Nanostar SAXS camera, with pinhole collimation for point focus geometry. The instrument source is a copper rotating anode (0.1 mm filament) operating at 50 kV and 24 mA, fitted with cross-coupled Göbel mirrors, resulting in a Cu Kα radiation wavelength of 1.54 Å. The SAXS camera is fitted with a Hi-star 2D detector (effective pixel size of 100 μm). The sample–detector distance was chosen to be 650 mm, which provided a q range from 0.02 to 0.3 $Å^{-1}$, where q is the magnitude of the scattering vector defined as

$$q = \frac{4\pi}{\lambda}\sin\theta$$

where λ is the wavelength and 2θ is the scattering angle. Starch slurries (45%, w/w) were presented in 2 mm glass capillaries. The optics and sample chamber were under vacuum to minimize air scatter. Scattering files were normalized to sample transmission, background-subtracted, and then radially averaged using macros written in the Igor software package (Wavemetrics, Lake Oswego, OR).

Table 2. Melting Temperature (T_m) and Melting Enthalpy (ΔH_m) of Retrograded Starch Fractions

samples		retrograded amylose endotherm peak		retrograded amylopectin endotherm peak	
		T_m (°C)	ΔH_m (J/g)	T_m (°C)	ΔH_m (J/g)
normal maize	control	145.5 (3.2)	2.0 (0.4)		
	4 °C	147.8 (0.9)	2.1 (2.0)		
	30 °C	148.7 (0.1)	0.9 (0.8)	46.5 (1.4)	2.4 (0.5)
	60 °C	146.8 (1.7)	0.7 (0.1)	53.4 (0.0)	1.0 (0.3)
high-amylose maize	control	145.3 (0.5)	2.5 (0.1)		
	4 °C	146.9 (2.4)	2.3 (0.2)		
	30 °C	146.9 (1.5)	1.0 (0.2)		
	60 °C	146.6 (2.2)	1.9 (0.1)		
waxy maize	control				
	4 °C				
	30 °C			44.0 (0.8)	0.4 (0.3)
	60 °C				
normal wheat	control	152.1 (1.0)	1.4 (0.4)		
	4 °C	158.0 (4.9)	1.7 (0.2)		
	30 °C	153.0 (1.0)	2.3 (1.3)	41.4 (1.5)	0.7 (0.1)
	60 °C	nd	nd	48.7 (3.5)	0.3 (0.1)

ERS Determination. ERS contents were determined by a procedure derived from Muir's method (*11*). In brief, to each 500 mg of powdered extrudates, 500 mg of artificial saliva (composed of 250 units of porcine pancreatic α-amylase in 1 mL of carbonate buffer at pH 7.0) was added. After 15–20 s, the mixture was incubated with 5 mL of acidified (0.02 M HCl) pepsin (1 mg/mL; Sigma) at 37 °C for 30 min, leading to a pH 2.0. The solution was then adjusted to pH 6.0 with 0.02 M NaOH, and the neutralized samples were treated with 5 mL of pancreatin/amyloglucosidase enzyme mixture for 16 h at 37 °C in 0.2 M acetate buffer at pH 6.0 in a shaking water bath. Samples were inactivated by adding an equal volume of 95% ethanol and centrifuged (2000*g* for 10 min). The supernatant was discarded, and the residue was washed twice, first with 0.2 M acetate buffer (pH 6.0), followed by water, and then freeze-dried. The resuspended pellet was homogenized, and its starch content was then determined by digesting with thermostable α-amylase and amyloglucosidase, from the method derived from the total starch assay using a kit from Megazyme (Megazyme International Ireland Ltd., Ireland). The glucose content was then determined by adding enzymatic glucose reagent and measuring the absorbance. A portion of the resuspended washed pellet was centrifuged and then freeze-dried for further structural analysis.

RESULTS

Characterization of the Processed Products. *Retrograded Amylose and Amylopectin by DSC.* The melting temperature and enthalpy of retrograded amylose and amylopectin were determined by DSC for the different starches just after processing (control samples) and after storage at 4, 30, and 60 °C and 17% moisture content. As previously described in the literature (*9*), melting of retrograded amylopectin takes place between 40 and 60 °C, while the melting peak of retrograded amylose is located at higher temperatures between 120 and 170 °C. DSC results for the different starches are presented in **Table 2** and show that normal maize starch, high-amylose maize starch, and wheat starch exhibit an endothermic peak located between 145 and 160 °C for each sample, independent of their storage conditions. However, the enthalpy of the peak was low and not significantly different from one sample to another (between 1 and 2.5 J/g). This peak, which disappears on a second scan, could be attributed to the melting of retrograded amylose. No retrograded amylose peak was observed for waxy maize materials, which was expected because the amylose content of this starch is low (3.5%). Peaks between 40 and 55 °C, attributed to retrograded amylopectin, were observed for normal maize, waxy maize, and normal wheat starch materials but only in the samples stored at 30 and 60 °C. Those peaks also disappeared on a second scan by DSC. The retrogradation kinetics of amylopectin is known to be quite different from those of amylose, with the amylopectin fraction of starch being responsible for long-term changes occurring during storage (*12*). It has been suggested that amylopectin molecules associate by crystallization of relatively short (DP ∼ 15) chain-length branches (*13*). The increased thermal energy imparted to the molecules at the higher storage temperatures could have contributed to an increased mobility of the amylopectin-branched chains, thus facilitating their reordering. Having said this, the extent of amylopectin retrogradation was low, demonstrated by the measured low enthalpies, which were not greater than 2.5 J/g, while in excess water, enthalpy values for amylopectin retrogradation have been observed to vary from ca. 8–12 J/g (*12*).

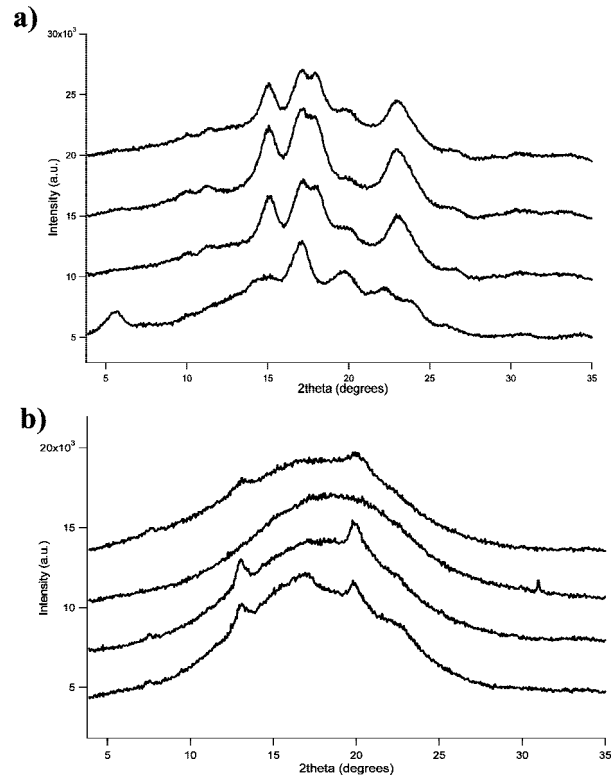

Figure 2. X-ray diffractograms of (a) raw and (b) processed starches. From top to bottom: wheat, waxy maize, normal maize, and high-amylose maize. Data have been offset for clarity.

Nanostructure of the Products. In **Figure 2**, the diffractograms of the raw and processed starch samples (control samples) are displayed. In agreement with previous studies (*14*), only the raw high-amylose maize starch shows a B-type crystallinity, while the other cereal samples, with less than 35% amylose content, have diffractograms typical of A-type crystal structures, with main reflections at $2\theta \sim 15°$, 23°, and a doublet with peaks at 17° and 18°.

Processing of the starches leads to the complete gelatinization of waxy maize and the additional formation of V-type crystallinity (reflections at $2\theta \sim 7°$, 13°, and 20°) in the other three starches (see **Figure 2b** corresponding to control samples). V-type crystals have been observed to be formed by single amylose helices complexed with different polar and nonpolar compounds, such as fatty acids (*15*). Nuclear magnetic resonance (NMR) analysis of native starches suggested that all intragranular lipids are present as complexes with glucan chains (*16*). It seems that extrusion leads to the parallel arrangement of these

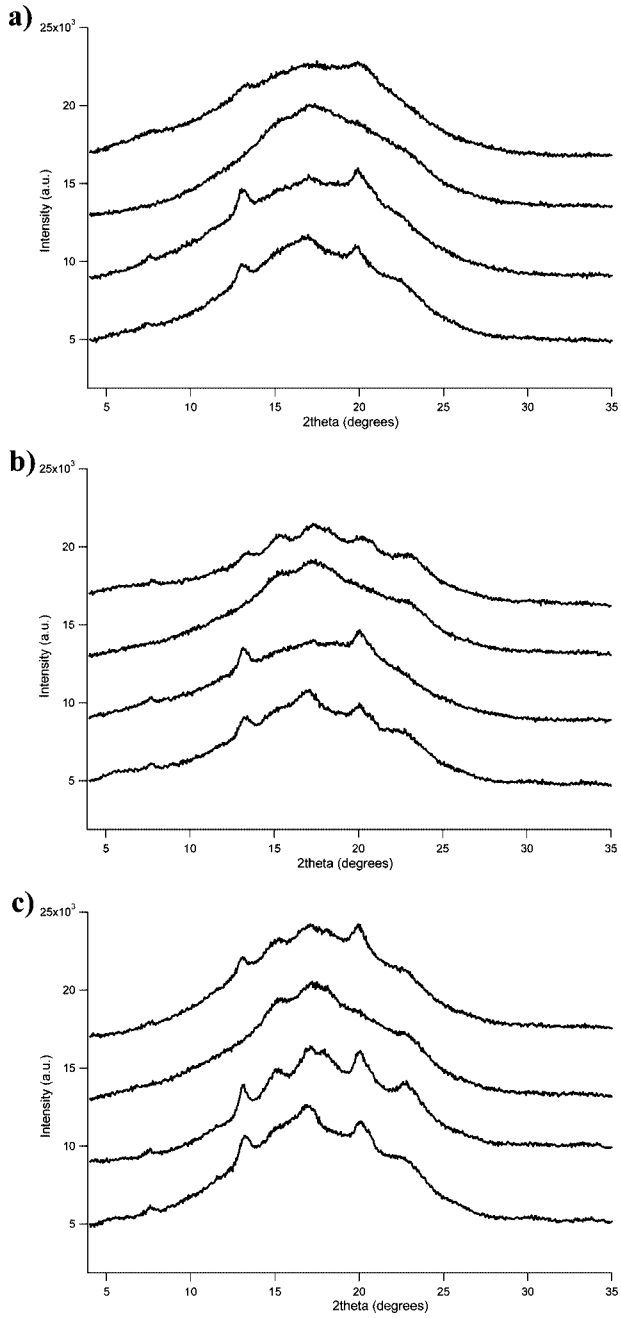

Figure 3. X-ray diffractograms of the processed starches after 72 h of storage at (a) 4, (b) 30, and (c) 60 °C. From top to bottom: wheat, waxy maize, normal maize, and high-amylose maize. Data have been offset for clarity.

amylose–lipid complexes, giving rise to the V-type structures observed in the diffractograms. Moreover, the higher the amylose content of the starch, the higher the crystallinity remaining following processing.

After 72 h of storage, the levels of crystallinity of the processed starches varied as a function of the storage temperature and starch type as shown in **Figure 3**.

After storage at 4 °C, the diffractograms of the different materials do not show significant differences, except in the case of the waxy maize, which, in contrast with the amorphous halo displayed for the control sample, shows some crystalline reflections. Amylopectin retrogradation requires high polysaccharide concentrations, with crystallites being formed by the relatively short branches of the molecule. The increase in crystalline material as indicated by the XRD data for waxy

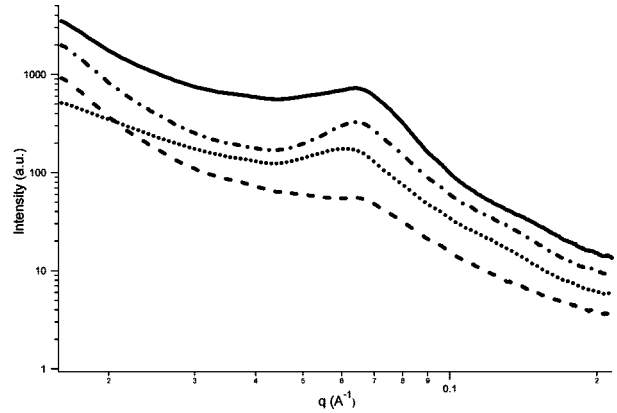

Figure 4. SAXS patterns of raw starches. From top to bottom: waxy maize (—), normal maize (- · -), wheat (· · ·), and high-amylose maize (- - -). Data have been offset for clarity.

Table 3. Intensity (I_{max}), Position (q_{max}), Bragg Spacing ($d = 2\pi/q$), and Full Width at Half-Maximum (Δq) of the SAXS Peak for the Wet Starches and Value of the Power Law Exponent (δ) Obtained from Fitting the Curves to eq 1

	I_{max} (a.u.)	q_{max} (Å^{-1})	d (nm)	Δq (Å^{-1})	δ
normal maize	391.3	0.063	9.9	0.038	3.5
high-amylose maize	271.6	0.059	10.6	0.049	3.1
waxy maize	425.7	0.061	10.3	0.027	2.7
normal wheat	417.2	0.060	10.5	0.037	2.4

maize is in accordance with classical polymer crystallization theories, where nucleation is favored at low temperatures, but less perfect crystals are expected to be formed as the degree of supercooling (relative to the melting temperature) increases (*17*).

After storage at 30 °C, the largest XRD changes relative to the control samples are observed for the wheat sample and the high-amylose maize starch (see **Figure 3b**), but in contrast with the observations from DSC, all materials exhibit a slight increase in crystallinity. However, in comparison to the raw starches (**Figure 2a**), the crystals formed in the wheat sample and, indeed, in all samples, at this storage temperature are less well-defined.

An enhancement in the crystalline structure and content takes place, as shown in **Figure 3c**, at the highest storage temperature (60 °C) for all starch samples studied. From the diffraction patterns, the type of crystals can be identified with an A-type structure prevailing for the waxy maize, a mixture of A and V forms for wheat and normal maize, and in the case of the high-amylose maize, both B- and V-type crystal reflections are observed.

SAXS was used to compare the initial crystalline order of the raw starches. In **Figure 4**, the SAXS curves corresponding to the four different starches studied are displayed. The parameters of the SAXS curves (intensity, I_{max}; position, q_{max}; and width of the peak at half-maximum, Δq) were obtained by fitting the data to the following equation:

$$I(q) = I_{max}[1 + (2(q - q_{max})/\Delta q)^2]^{-1} + Aq^{-\delta} \qquad (1)$$

The first term in eq 1 is the Lorentz function, which describes the SAXS peak, while the second term is a power law function to account for the underlying diffuse scattering, where A is a prefactor and δ is the power law exponent. The fitting parameters obtained for the raw starches are shown in **Table 3**, and **Figure 5** shows, as an example, the fit obtained for wheat.

Every raw material shows the characteristic peak at $q \sim 0.07$ Å^{-1}, which corresponds to the typical ~9–10 nm lamellar repeat

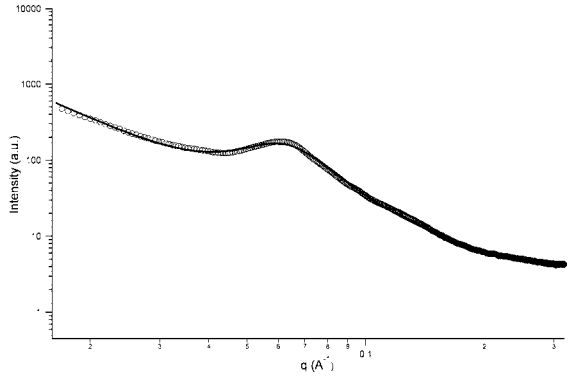

Figure 5. SAXS curve for raw wheat. Experimental data (○) and associated fit to eq 1 (—).

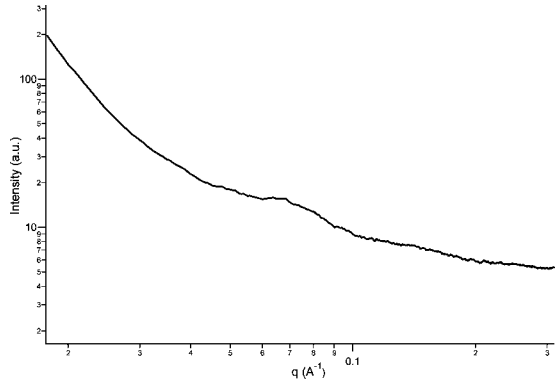

Figure 6. SAXS pattern of extruded waxy maize (control sample).

of starch architecture within the granule (thickness of crystalline plus amorphous regions of the lamella). From the values in **Table 3** and in agreement with previous studies (*18*), it seems that an increase in amylose content leads to a decrease in the intensity of the scattering maximum (I_{max}). According to the XRD theory (*18*), I_{max} depends upon the amount of the ordered semicrystalline structures and/or the differences in electron density between crystalline and amorphous lamellae within the starch granules. It has been suggested that the amylose chains could act as defects in the crystalline lamellae (*19*); this would also explain the increase in the width at half-maximum of the SAXS peak with an increasing amylose content (see **Table 3**).

Surprisingly, despite the original crystallinity of the samples being mostly eliminated during processing (cf. parts a and b of **Figure 2**), the 9–10 nm repeat typical of raw starches is still present in the SAXS patterns of the control samples (cf. **Figures 4** and **6**), although the intensity of the peaks is obviously much lower. Even the waxy maize starch, which after extrusion shows an amorphous diffractogram, displays the characteristic reflection as shown in **Figure 6**. Waigh et al. (*20*) found that, when heating starch in excess water, the SAXS peak disappeared essentially at the same temperature as the WAXS peak. However, the relatively low water content used during processing in this work may have prevented the expansion of chains that accompany the smectic–gel transformation in excess water.

During storage, the formation of crystals is reflected by the appearance of a shoulder in the SAXS patterns. In contrast with the peak observed in the raw starches, the peak in the stored starches reflects molecular reorganization and extends over a broad q range, indicating the formation of a heterogeneous semicrystalline structure. An example of the SAXS pattern obtained after storage will be shown below, together with the SAXS patterns for the ERS fractions.

Table 4. Crystallinity Content (Xc), Amount of V-Type Crystallinity, and ERS Content of the Different Starches before and after Processing and Storage at Different Temperatures (17% MC)

		Xc (%)	V type (%)	ERS (%)[a]
	raw	26.1	2.1	0.8
	control	2.9	2.9	2.8
wheat	4 °C	3.2	2.6	2.7
	30 °C	6.3	1.8	3.2
	60 °C	5.8	2.6	3.2
	raw	43.5	1.0	0.7
	control			0.1
waxy maize	4 °C	3.5		0.1
	30 °C	5.1		0.0
	60 °C	6.6		0.0
	raw	32.2	3.1	1.5
	control	4.0	4.0	2.1
normal maize	4 °C	6.5	2.7	2.6
	30 °C	6.7	2.7	3.4
	60 °C	11.7	3.2	3.2
	raw	23.4	3.6	69.6
	control	7.8	2.8	20.0
high-amylose maize	4 °C	8.8	2.8	23.0
	30 °C	11.2	2.5	25.2
	60 °C	13.8	3.1	27.3

[a] Standard deviation of 0.3.

ERS Content. The amount of ERS was determined for the various raw, processed, and stored samples (**Table 4**). The ERS content of the native starches varied as a function of the composition and origin, i.e., for maize starches, the higher the amylose content, the higher the ERS content, but for similar amylose/amylopectin composition, normal maize contained a larger fraction of ERS than wheat. Similar results were obtained by Ring et al. (*4*), who quantified the rate and extent of α-amylase hydrolyzis of starches from different botanical sources. They observed a higher degree of hydrolyzis for wheat, which seemed to be correlated with the granule size, i.e., smaller granules have greater surface area per unit volume for enzyme attack. Other factors, such as the granule architecture, also influence the resistance to amylolysis of granular starch (*21, 22*).

After processing, a slight increase in ERS content was observed for wheat and normal maize, up to 3.2% for the samples stored at 60 °C. The ERS content of waxy maize, on the other hand, was reduced to zero when processed. Greater amounts of ERS after processing were obtained for the high-amylose maize starch, although the amount of ERS was reduced in comparison to the raw material.

In general, the ERS content of the different starches did not significantly increase upon storage. The only sample that showed an increase in parallel with the crystallinity increase was high-amylose maize starch, which showed a ERS content of ∼27% after conditioning at 60 °C, compared to the 20% obtained for the control.

For every starch type studied, there was no correlation between the endothermic enthalpies measured at 145 °C by DSC (which have been associated with amylose that has undergone a retrogradation process) and the ERS content. It is also clear from the XRD data that there appears to be no correlation between the crystallinity content of the starch samples before enzymatic digestion and the ERS content measured. This suggests that the digestion process itself is very important when considering the mechanisms of ERS formation and, therefore, warrants further research attention.

Residual Structure of the ERS. The ERS structure was studied for the high-amylose maize starch, because the low percentages of ERS obtained for the other starches made an accurate structure determination unreliable.

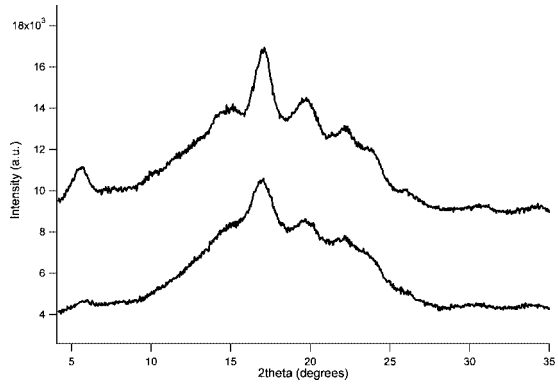

Figure 7. X-ray diffractograms for raw high-amylose maize before (upper curve) and after *in vitro* digestion (lower curve). Data have been offset for clarity.

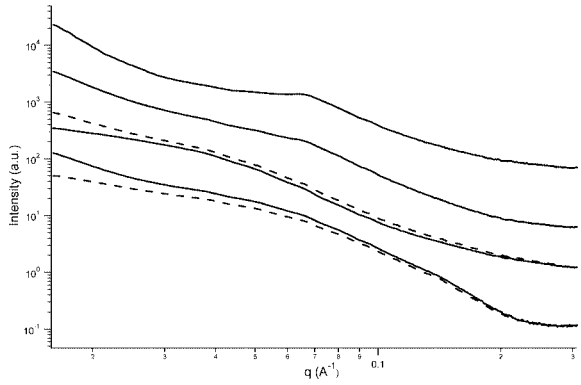

Figure 8. SAXS patterns of high-amylose maize. From top to bottom: raw starch, ERS fraction of raw starch, control sample (- - -) overlapping with the sample stored at 60 °C, and ERS fractions of the control sample (- - -) and starch stored at 60 °C. Data have been offset for clarity.

The diffractogram of the ERS fraction left after digestion of granular high-amylose starch shows less intense and defined peaks (see **Figure 7**), indicating a reduction in both crystallinity and crystal perfection. This observation confirms that crystallinity alone cannot explain the resistance to digestion. The crystalline polymorph of the ERS fraction is the same as in native starch, in agreement with previous studies dealing with the digestion of native starches (*23*).

SAXS was used to analyze the ERS fractions of the native and processed high-amylose starch. In **Figure 8**, the SAXS curves before and after digestion of high-amylose starch raw, processed, and stored at 60 °C are displayed. Digestion of the raw starch does not substantially alter lamellar order, because the ~9–10 nm lamellar scattering peak is still observed in the ERS fraction. However, the intensity of this peak is even lower, which agrees with the XRD results and means that this fraction has a lower crystalline order than the native material. After processing, the structure of the starch is substantially changed and the lamellar peak is replaced by a broad reflection. In comparison to the control (- - -) with the sample stored at 60 °C, it is seen that, in the former, the broad reflection extends over a larger q range, which means that storing the sample at a higher temperature causes annealing and reorganization of the crystals present, therefore suggesting a more homogeneous crystalline structure.

In the SAXS curves of the ERS fractions, the broad reflection is shifted toward higher q, i.e., shorter distances, which indicates that the distance between two consecutive crystalline regions is smaller, although the semicrystalline structure is still quite heterogeneous as indicated by the peak width. The increase in low-angle scattering for the sample stored at 60 °C may also indicate the formation of a larger scale structure.

DISCUSSION

DSC is an extremely useful tool for the analysis of thermal transitions in polymeric materials, but in the case of starch, this technique is insufficient to monitor all of the structural changes taking place during the processing and storage of this biopolymer. Jenkins and Donald (*24*) determined that more than 20% of total crystallinity, as revealed by XRD, remained after wheat, potato, corn, tapioca, and pea starches were heated past the endotherm conclusion temperature observed by DSC. Apart from the inaccuracy in the determination of the gelatinization range, apparent from the high standard deviation values, in this work, it is demonstrated that starch retrogradation is better followed by X-ray diffraction. DSC, on the other hand, has been useful to distinguish between amylose and amylopectin retrogradation.

In **Table 4**, the crystallinity values for the different samples are displayed. It can be observed that the higher the amylose content of the granules, the lower the crystallinity of the raw materials. This is easily understood taking into account that the amylopectin fraction is predominantly responsible for the crystalline arrangement in native starches (*25*). In this table, the percentage of V-type crystallinity is also displayed. The peak at $2\theta \sim 20°$ has been typically attributed to amylose–lipid complexes in raw starches. From the values shown in the table, it is seen that the higher the amylose content of the sample, the higher the contribution of this peak to the crystallinity. The contribution of this reflection in native waxy maize starch is very low, as expected.

From XRD, it has also been observed that cereal starches with high-amylose content are more resistant to gelatinization during processing than normal or high amylopectin ones (see **Figure 2b** for control samples), as well as having higher levels of enzyme resistance. This can partly be explained by the type of crystalline polymorph, i.e., B- (and C-) type crystalline structures being more resistant to α-amylase hydrolyzis than A-type crystalline structures (*21*, *23*). Further confirmation of the higher resistance of the B-type crystal structure to enzymatic degradation was gained using lintner residues of starches (*26*) and preparing A- and B-type polymorphs from amylose (*27*). Moreover, it has been observed (*28*) that native cereal starches during digestion have a high "slow digestible" fraction (~50%), meaning that, if some granules remain ungelatinized during processing, they will increase the amount of slowly digestible starch with the health-related benefits associated with this fraction (*29*). Recently, it has been suggested that amylose located in the amorphous regions of the granule could rearrange, forming new intermolecular bonds during the first stages of gelatinization (*30*), which could also explain the higher resistance to gelatinization with increasing amylose content. This process has been ascribed to the entrance of water into the granule, causing swelling and favoring polymer mobility.

Furthermore, processing under limited water conditions (28% MC) leads to the formation of amylose single helices, as can also be observed in **Figure 2b**. It has been suggested that processing (*31*) and, more specifically, extrusion (*32*) may increase the formation of amylose–lipid complexes and thus reduce starch digestibility. The complex resulting from the interaction between starch and lipids is particularly important because it modifies the texture and structural stability of starch-based products (*33*). In this work, an increase in the percentage of amylose single helices has been observed after extrusion of

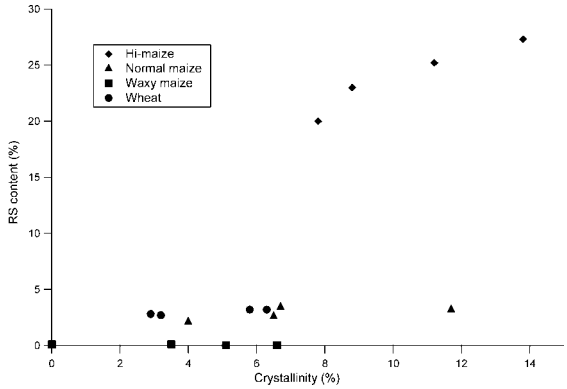

Figure 9. ERS content of extruded samples versus crystallinity developed during conditioning.

wheat and normal maize, both with medium amylose contents (see the percentage of V-type values in **Table 4**). In the case of the high-amylose starch, the amount of V-type crystallinity is reduced in comparison to the fraction present in the native material, while waxy maize starch processing leads to a complete gelatinization of the samples, as observed from the amorphous XRD pattern (see **Figure 2b**).

Upon storage, retrogradation takes place in every starch studied and is favored at the highest storage temperature. However, the amount of recrystallization is quite limited, which can be explained from a glass transition temperature (T_g) viewpoint. At 17% water content, extruded starch would have a T_g around 39 °C, as predicted by Bindzus et al. (*34*) and, therefore, at the temperatures used for conditioning starch, chain mobility will be quite restricted. In **Figure 9**, the crystallinity content of the different processed and stored starches is shown versus their ERS content. From this figure, it can be inferred that the increase in crystallinity as a consequence of storage is not directly correlated with an increase in ERS. In fact, the only sample that shows a significant increase in ERS content upon storage is high-amylose starch. The fact that retrograded amylopectin is completely degraded by α-amylase (*4*) would explain the null values of ERS for the waxy maize, but as with native starches, crystallinity alone cannot explain resistance to digestion. This novel result contrasts with the previous understanding of the origin of ERS from processed starches, which considered this fraction to result from amylose recrystallization, subsequent to gelatinization, into enzyme-resistant double helices stabilized by hydrogen bonds and characterized by a high thermal stability (*35*–*37*). It should be remembered that these findings are, up to now, limited to *in vitro* generated ERS.

With regard to the ERS fractions, from **Figure 8**, it is observed that the structures left after *in situ* digestion are quite different if the starch has been processed. The conditions of digestion (water and temperature) are expected to allow for the retrogradation and annealing of the existing crystals. In previous work (*38*), an increased crystallinity in the ERS fractions from processed starches suggested that some retrogradation took place during digestion, with the resistance to digestion being determined by the competition between the kinetics of enzymatic hydrolyzis and the kinetics of amylose reorganization. In **Figure 8**, a shift of the SAXS broad reflection after digestion is observed from $q \sim 0.04$ Å^{-1} to 0.07 Å^{-1}, i.e., from ~16 to ~9 nm. This characteristic length is often referred to as the long period (L) and corresponds to the average thickness of the amorphous plus the crystalline lamellae. Jane and Robyt (*39*), on the basis of chromatography studies on retrograded amylose using various amylases and sulfuric acid to hydrolyze the amorphous regions, proposed a structural model consisting of double-helical regions of ~10 nm long interspersed with amorphous regions. Cagiao and co-workers (*40*) studied the retrogradation of injection-molded potato starch during annealing and determined that the first crystals appearing from the gelatinized structure are the largest ones and, with an increasing temperature, a decrease in crystal size takes place until a value of $L \sim 6$ nm is reached. This decrease in the long period has been ascribed to the growth of thin crystals inside or outside the lamellar stacks. This same process seems to be taking place during digestion of the high-amylose starch, and the only noticeable difference between the SAXS patterns of the control sample and that stored at 60 °C is that the latter one shows a more defined peak and, therefore, a less heterogeneous structure.

The *in vitro* method used for the quantification of the ERS fractions left after digestion of the various starches is a modification of Muir's method aimed at providing satisfactory and reproducible predictions of the fractions obtained *in vivo*. The values obtained (see **Table 4**) are an average of two digestion experiments, and they showed a standard deviation of 0.3, confirming the reliability of the method. From **Table 4**, it is apparent that except for high-amylose starch, storage of the samples and subsequent increase in the crystallinity does not increase the amount of ERS.

Therefore, retrogradation prior to digestion could increase the resistance to digestion of high-amylose starches but, as demonstrated in this work, does not have a significant impact on normal or waxy starches. Furthermore, in the case of high-amylose starch, the crystallinity values before digestion cannot be directly correlated with the percentage of ERS obtained, suggesting that there are additional mechanisms involved in the formation of these resistant fractions. Therefore, a closer investigation of the structural changes ocurring during digestion would be of significant interest to enable a much deeper understanding of ERS formation.

ACKNOWLEDGMENT

We thank Tracey Hanley for her assistance with the SAXS experiments, Cecile Apel for technical laboratory assistance, and Tony Bird for kindly providing the method for the *in vitro* ERS assessment.

LITERATURE CITED

(1) Tapsell, L. C. Diet and metabolic syndrome: Where does resistant starch fit in? *J. AOAC Int.* **2004**, *87*, 756–761.
(2) Topping, D. L.; Clifton, P. M. Short-chain fatty acids and human colonic function: Roles of resistant starch and nonstarch polysaccharides. *Pharmacol. Rev.* **2001**, *81*, 1031–1064.
(3) Brown, I. L.; McNaught, K. J.; Moloney, E. Hi-maize: New directions in starch technology and nutrition. *Food Aust.* **1995**, *47*, 272–275.
(4) Ring, S. G.; Gee, J. M.; Whittam, M.; Oxford, P.; Johnson, I. T. Resistant starch: Its chemical form in foodstuffs and effect on digestibility in vitro. *Food Chem.* **1988**, *28*, 97–109.
(5) Swinkels, J. J. M. Sources of starch, its chemistry and physics. In *Starch Conversion Technology*; van Beynum, G. M. A., Roels, J. A., Eds.; Marcel Dekker: New York, 1985; pp 15–46.
(6) Khana, S.; Tester, R. F. Influence of purified konjac glucomannan on the gelatinization and retrogradation properties of maize and potato starches. *Food Hydrocolloids* **2006**, *20*, 567–576.
(7) Kim, J. H.; Tanhehco, E. J.; Ng, P. K. W. Effect of extrusion conditions on resistant starch formation from pastry wheat flour. *Food Chem.* **2006**, *99*, 718–723.
(8) Cui, R.; Oates, C. G. The effect of retrogradation on enzyme susceptibility of sago starch. *Carbohydr. Polym.* **1997**, *32*, 65–72.

(9) Leeman, A. M.; Karlsson, M. E.; Eliasson, A. C.; Björck, I. M. E. Resistant starch formation in temperature treated potato starches varying in amylose/amylopectin ratio. *Carbohydr. Polym.* **2006**, *65*, 306–313.
(10) Chrastil, J. Improved colorimetric determination of amylose in starches or flours. *Carbohydr. Res.* **1987**, *159*, 154–158.
(11) Muir, J.; Birkett, A.; Brown, I.; Jones, G.; O'Dea, K. Food processing and maize variety affects amounts of starch escaping digestion in the small intestine. *Am. J. Clin. Nutr.* **1995**, *61*, 82–89.
(12) Fredriksson, H.; Silverio, J.; Andersson, R.; Eliasson, A. C.; Aman, P. The influence of amylose and amylopectin characteristics on gelatinization and retrogradation properties of different starches. *Carbohydr. Polym.* **1998**, *35*, 119–134.
(13) Ring, S. G.; Colonna, P.; L'Anson, K. J.; Kalichevsky, M. T.; Miles, M. J.; Morris, V. J.; Orford, P. D. The gelation and crystallization of amylopectin. *Carbohydr. Res.* **1987**, *162*, 277–293.
(14) Cheetam, N. W. H.; Tao, L. Variation in crystalline type with amylose content in maize starch granules: An X-ray powder diffraction study. *Carbohydr. Polym.* **1998**, *36*, 277–284.
(15) Godet, M. C.; Bouchet, B.; Colonna, P.; Gallant, D. J.; Buleon, A. Crystalline amylose–fatty acid complexes: Morphology and crystal thickness. *J. Food Sci.* **1996**, *61*, 1196–1201.
(16) Morrison, W. R.; Tester, R. F.; Snape, C. E.; Law, R.; Gidley, M. J. Swelling and gelatinization of cereal starches. 4. Some effects of lipid-complexed amylose and free amylose in waxy and normal barley starches. *Cereal Chem.* **1993**, *70*, 385–391.
(17) Wunderlich, B. In *Macromolecular Physics: Crystal Growth, Annealing*; Academic Press: New York, 1976.
(18) Yuryev, V. P.; Krivandin, A. V.; Kiseleva, V. I.; Wasserman, L. A.; Genkina, N. K.; Fornal, J.; Blaszczac, W.; Schiraldi, A. Structural parameters of amylopectin clusters and semi-crystalline growth rings in wheat starches with different amylose content. *Carbohydr. Res.* **2004**, *339*, 2683–2691.
(19) Feigin, L. A.; Svergun, D. I. In *Structure Analysis by Small-Angle X-ray and Neutron Scattering*; Plenum: New York, 1987.
(20) Gallant, D. J.; Bouchet, B.; Buleon, A.; Perez, S. Physical characteristics of starch granules and susceptibility to enzymatic degradation. *Eur. J. Clin. Nutr.* **1992**, *46*, S3–S16.
(21) Waigh, T. A.; Gidley, M. J.; Komanshek, B. U.; Donald, A. M. The phase transformation in starch during gelatinization: A liquid crystalline approach. *Carbohydr. Res.* **2000**, *328*, 165–176.
(22) Fannon, J. E.; Gray, J. A.; Gunawan, N.; Huber, K. C.; BeMiller, J. N. Heterogeneity of starch granules and the effect of granule channelisation on starch modification. *Cellulose* **2004**, *11*, 247–254.
(23) Gerard, C.; Colonna, P.; Buleon, A.; Planchot, V. Amylolysis of maize mutant starches. *J. Sci. Food Agric.* **2001**, *81*, 1281–1287.
(24) Jenkins, P. J.; Donald, A. M. Gelatinization of starch: A combined SAXS/WAXS/DSC and SANS study. *Carbohydr. Res.* **1998**, *308*, 133–147.
(25) Waigh, T. A.; Kato, K. L.; Donald, A. M.; Gidley, M. J.; Clarke, C. J.; Riekel, C. Side-chain liquid-crystalline model for starch. *Starch/Staerke* **2000**, *52*, 450–460.
(26) Planchot, V.; Colonna, P.; Buleon, A. Enzymatic hydrolysis of glucan crystallites. *Carbohydr. Res.* **1997**, *298*, 319–326.
(27) Williamson, G.; Belshaw, N. J.; Self, D. J.; Noel, T. R.; Ring, S. G.; Cairns, P.; Morris, V. J.; Clark, S. A.; Parker, M. L. Hydrolysis of A-type and B-type crystalline polymorphs of starch by α-amylase, *β*-amylase and glucoamylase-1. *Carbohydr. Polym.* **1992**, *18*, 179–187.
(28) Zhang, G.; Ao, Z.; Hamaker, B. R. Slow digestion property of native cereal starches. *Biomacromolecules* **2006**, *7*, 3252–3258.
(29) Ludwig, D. D. S. The glycemic index. Physiological mechanisms relating to obesity, diabetes and cardiovascular disease. *J. Am. Med. Assoc.* **2002**, *287*, 2414–2423.
(30) Ratnayake, W. S.; Jackson, D. S. A new insight into the gelatinization process of native starches. *Carbohydr. Polym.* **2007**, *67*, 511–529.
(31) Jacobs, H.; Delcour, J. A. Hydrothermal modifications of granular starch with retention of the granular structure: A review. *J. Agric. Food Chem.* **1998**, *46*, 2895–2905.
(32) Asp, N. G.; Björk, I. Nutritional properties of extruded foods. In *Extrusion Cooking*; Mercier, C., Linko, P., Harper, J. M., Eds.; American Association of Cereal Chemists (AACC): St. Paul, MN, 1989; pp 399–434.
(33) Georgopoulos, T.; Larsson, H.; Eliasson, A. C. Influence of native lipids on the rheological properties of wheat flour dough and gluten. *J. Texture Stud.* **2006**, *37*, 49–62.
(34) Bindzus, W.; Livings, S. J.; Gloria-Hernandez, H.; Favard, G.; van Lengerich, B.; Meuser, F. Glass transition of extruded wheat, corn and rice starch. *Starch/Staerke* **2002**, *54*, 393–400.
(35) Englyst, H. N.; Kingman, S. M.; Cummings, J. H. Classification and measurement of nutritionally important starch fractions. *Eur. J. Clin. Nutr.* **1992**, *46*, S33–S50.
(36) Haralampu, S. G. Resistant starch—A review of the physical properties and biological impact of RS3. *Carbohydr. Polym.* **2000**, *41*, 285–292.
(37) Thompson, D. B. Strategies for the manufacture of resistant starch. *Trends Food Sci. Technol.* **2000**, *11*, 245–253.
(38) Lopez-Rubio, A.; Htoon, A.; Gilbert, E. P. The influence of extrusion and digestion on the nanostructure of high-amylose starches. *Biomacromolecules* **2007**, *8*, 1564–1572.
(39) Jane, J.-L.; Robyt, J. F. Structure studies of amylose-V complexes and retrograded amylose by action of α-amylases, and a new method for preparing amylosdextrins. *Carbohydr. Res.* **1984**, *132*, 105–118.
(40) Cagiao, M. E.; Rueda, D. R.; Bayer, R. K.; Balta Calleja, F. J. Structural changes of injection molded starch during heat treatment in water atmosphere: Simultaneous wide and small-angle X-ray scattering study. *J. Appl. Polym. Sci.* **2004**, *93*, 301–309.

Received for review July 3, 2007. Revised manuscript received September 20, 2007. Accepted September 27, 2007.

JF071974E